

Synthesis, Reactivity and DFT Investigation of a Cationic Zirconocene Benzyl Compound with an Appended Phenyl Group

Jörg Saßmannshausen,^{*,[a]} Anna Track,^[a] and Tiago A. D. S. Dias^[b]

Dedicated to M. L. H. Green

Keywords: Density functional calculations / NMR spectroscopy / Polymerisation

The reaction of $[\eta^5\text{-C}_5\text{H}_5\text{-(}\eta^5\text{-C}_5\text{H}_4\text{CMe}_2\text{C}_6\text{H}_4\text{Me)Zr(CH}_2\text{Ph)}_2]$ (**1**) with the cation generating agent $\text{B(C}_6\text{F}_5)_3$ was studied by means of multinuclear NMR and density functional theory (DFT) methods. The clean reaction in CD_2Cl_2 at -60°C yielded the cationic compound $[\eta^5\text{-C}_5\text{H}_5\text{-(}\eta^5\text{:}\eta^1\text{-C}_5\text{H}_4\text{-CR}_2\text{C}_6\text{H}_4\text{R)Zr}(\eta^2\text{-CH}_2\text{Ph)}]$ ($\text{R} = \text{Me}$: **2**, $\text{R} = \text{H}$: **3**), with a tolyl moiety coordinated to the cationic zirconium centre, in addition to the expected η^2 -coordination of the benzyl moiety. Both coordinations were unambiguously assigned by multi-

nuclear one- and two-dimensional NMR spectroscopy. Detailed DFT calculations of congener **3** at the B3LYP level of theory explain the unusual chemical shift of the coordinated atom of the tolyl moiety. Furthermore, detailed electronic analysis (Bader and NBO analysis) were undertaken to ascertain the type of coordination (agostic versus electrostatic) that the tolyl moiety adopts.

(© Wiley-VCH Verlag GmbH & Co. KGaA, 69451 Weinheim, Germany, 2007)

Introduction

Group 4 metallocenes are still a point of research interest as they can serve not only as the catalyst in hydrosilylation and hydration reactions, but they are also well known for their ability to polymerise monomers such as ethene, propene and styrene. In the last decades, much effort, both experimentally and theoretically,^[1–5] was undertaken to elucidate the role and the nature of the active species in these polymerisation reactions; thus, we have obtained a reasonably good picture of the catalytic process.^[6–15] The interaction of the cationic group 4 metallocene, which is accepted as the active species in the catalytic process, with both the neutral catalytic precursor and the anion has been extensively studied.^[6,7,9,14] The role of the solvent has been, by comparison, less investigated. Some time ago, we started to develop suitable models for the role of the solvent and showed by low-temperature NMR studies that arenes can coordinate to the cationic metal centre (compound **4**).^[16,17] We were also the first to report the formation of a zirconocene *dication*, such as **5**, which is stabilised by intra-

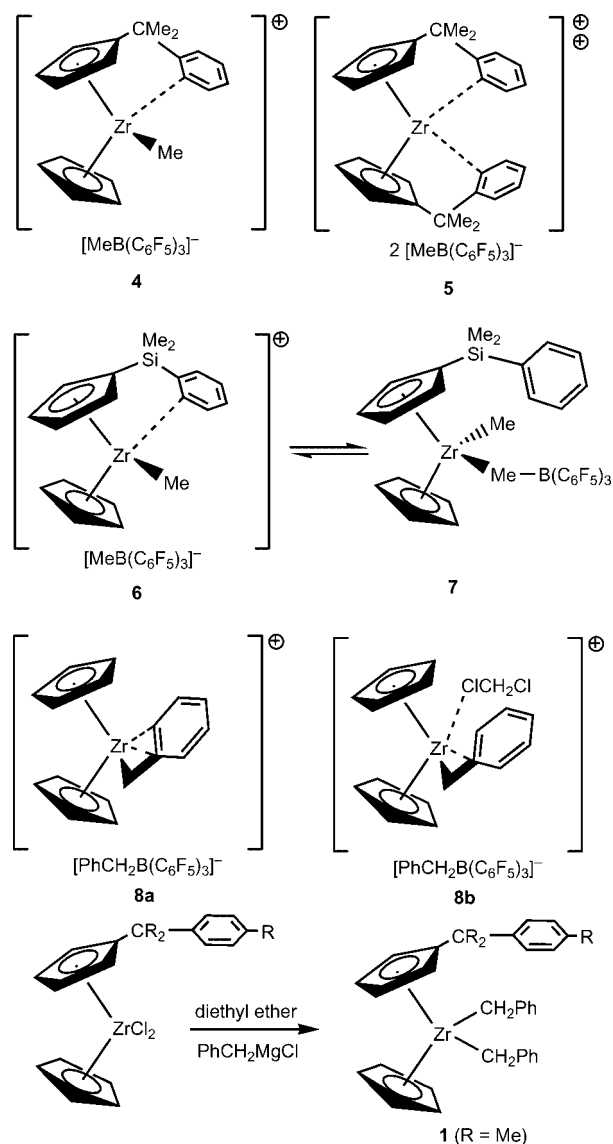
molecular phenyl coordination (Scheme 1).^[18] Recently, we extended this model and used silicon, instead of carbon, as a bridging atom. Here we noticed the formation of two different compounds: the expected formation of zirconocene compound **6**, which is in equilibrium with inner sphere ion pair **7**.^[19] Furthermore, we obtained evidence for the formation of dichloromethane adducts in the case of cationic zirconocene *benzyl* compounds **8a,b** and explored the electronic properties by DFT calculations.^[20]

As mentioned above, group 4 compounds are also used as catalysts for the polymerisation of styrene.^[21–23] Recently, Jo et al. demonstrated that in the case of *ansa*-titanocene compounds, secondary insertion of styrene, albeit slower than primary insertion, is actually the process that leads to the formation of polystyrene.^[24] One of the identified interim products was a metallocene benzyl compound. With this background, we decided to prepare compound **1** as a precursor to cation **2** to address the following: (1) the possible coordination of the pendant tolyl group, and, if this happens, (2) the nature of the coordination mode of the tolyl group (agostic versus electrostatic). To demonstrate the usability of our model, we firstly report the DFT calculations of **3**, and secondly we discuss the experimentally obtained NMR spectroscopic data of **2** (Scheme 2). Although this might be seen as an unusual way to present the obtained results, we believe that this way not only emphasises the validation of our model systems, but also allows the NMR results to be more easily understood.

[a] TU Graz, Institute for Chemistry and Technology of Organic Materials, Stremayrgasse 16/I, 8010 Graz, Austria
E-mail: sassmannshausen@tugraz.at

[b] Universidade do Minho, Department of Chemistry, Campus de Gualtar, 4710-057 Braga, Portugal

Supporting information for this article is available on the WWW under <http://www.eurjic.org> or from the author.



Scheme 1.

Scheme 2.

Results and Discussion

DFT Calculations

Structural Investigation

To save computational time, we substituted the *para* methyl group of the tolyl moiety in **2** with hydrogen, thus converting the tolyl moiety into a phenyl moiety to give **3** (Scheme 2).

We explored the possibility of different coordination modes of both the benzyl and the phenyl moiety to the cationic zirconium centre, and hence, calculated various conformers of **3**. A thorough scan of the potential energy surface revealed that **3a** is the global minimum of all considered coordination modes and that it is in rapid equilibrium with **3b** as confirmed by low-temperature NMR spectroscopy (Figure 1). Significant bond lengths, angles and dihedral angles are summarised in Table 1; the remaining energetically-higher-lying conformers are summarised in Table 2.

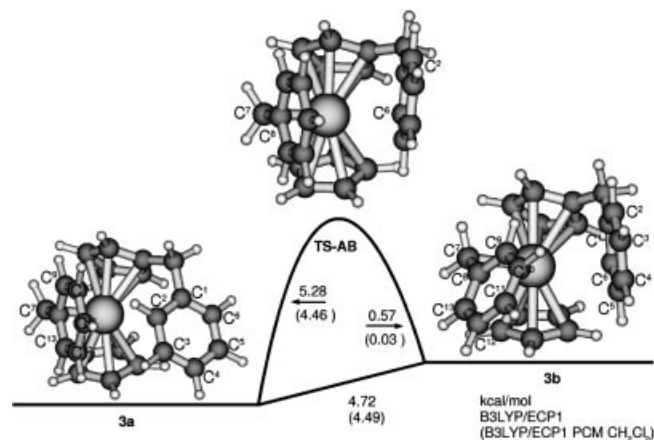


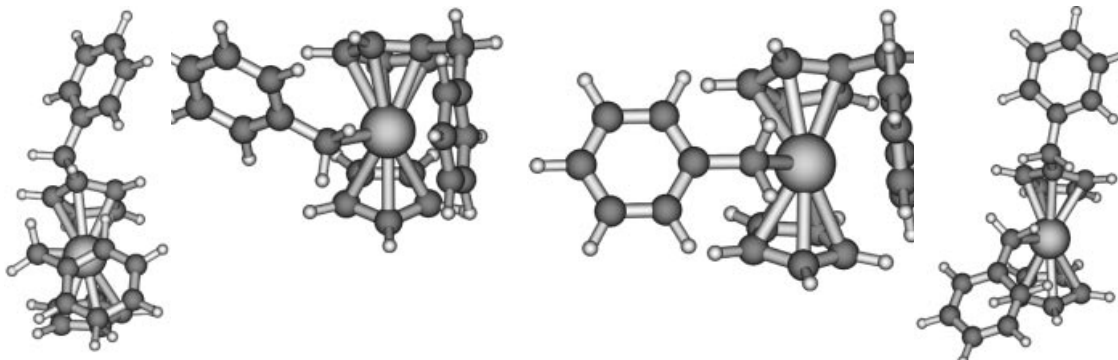
Figure 1. Scan of the potential energy surface of **3**. Values in parenthesis are calculated energies with the PCM solvent model (see text).

Table 1. Significant bond lengths, angles and dihedral angles of **3a** and **3b**.

	3a	TS-AB	3b
$d(\text{Zr}-\text{C}^7)$	2.33 Å	2.32 Å	2.34 Å
$d(\text{Zr}-\text{C}^8)$	2.71 Å	2.71 Å	2.71 Å
$d(\text{Zr}-\text{C}^2)$	2.92 Å	4.60 Å	—
$d(\text{Zr}-\text{C}^6)$	—	3.02 Å	3.16 Å
$\angle(\text{Zr}-\text{C}^7-\text{C}^8)$	87.7°	88.2°	87.5°
$\angle(\text{Zr}-\text{C}^7-\text{C}^8-\text{C}^9)$	95.5°	93.74°	61.2°

Here, the benzyl-moiety is bonded in an η^2 fashion to the zirconium centre and the phenyl moiety is coordinated in the previously described η^1 mode to the metal.^[16,17,25] The $\text{Zr}-\text{C}^7-\text{C}^8-\text{C}^9$ dihedral angle of 95.5° indicates symmetric coordination, with only a small distortion that is probably caused by the coordinated phenyl moiety. As previously reported,^[16,19] the hydrogen attached to the coordinated carbon of the phenyl moiety is bent out of the phenyl plane by 9.62° , away from the zirconium metal. A second minimum, **3b**, which is 4.72 kcal/mol higher in energy than **3a**, was obtained by coordination of the second *ortho* carbon of the phenyl moiety to the zirconium centre. Here, the benzyl moiety is slanted significantly ($\text{Zr}-\text{C}^7-\text{C}^8-\text{C}^9 = 61.2^\circ$) towards the metal and adopts an η^3 coordination to the metal centre. The phenyl moiety, which now points towards the “back” of the metallocene wedge, presumably leaves more space on the “front”; hence, the benzyl moiety

Table 2. Energetically higher lying conformers of **3**.

				
	3c	3d	3e	3f
Energy relative to 3a [kcal/mol]	6.65	7.18	7.38	

can adopt a coordination mode more suitable to satisfy the electron-deficient cationic metal centre. A similar coordination of cationic zirconocene benzyl compounds has been observed before.^[20] In the absence of coordinating solvents such as dichloromethane, we recently reported the formation of an η^3 -coordinated benzyl moiety to the cationic metallocene centre, compound **8a** ($\text{Zr}-\text{C}^7-\text{C}^8-\text{C}^9 = 51.8^\circ$). The addition of one molecule of dichloromethane furnished compound **8b** (cf. Scheme 1). Although in **3b** the electron deficiency of the metal is somehow compensated as a result of the coordination of the phenyl moiety, it is still strong enough to force the benzyl moiety into an η^3 coordination, albeit the slanting angle is about 10° smaller than that in **8a**. Further exploration of the potential energy surface furnished compounds **3c–e**. The last considered structure, **3f**, with no coordination of the benzyl or tolyl moiety, could not be obtained without restricted rotation of the $\text{Zr}-\text{CH}_2$ bond. In all calculations performed, the benzyl moiety had a strong tendency to move towards the metal centre to yield structures similar to **3c**. To investigate any possible solvent effects, we computed single-point calculations for the optimised energy structures, including the polarisable continuum model (PCM) solvent model implemented in GAUSSIAN03, with dichloromethane as a solvent. In general, the calculated single-point energies are somewhat lower than the solvent-free calculations, and the largest difference was 0.82 kcal/mol (Figure 1, values in parenthesis).

The small energy difference between **3a** and **3b** is important for styrene polymerisation: the incoming monomer (the tolyl group in our model) is attracted by the cationic metal centre and can coordinate to the free coordination site. This coordination can be envisaged for any of the conformers of **3**. However, as the energy barrier of rearrangement between any of the conformers is sufficiently small, the styrene monomer can move into a position so that the C–C double bond adopts a suitable position for insertion to occur.

Electronic Structure Investigations

To ascertain the coordination mode (agostic versus electrostatic) of the phenyl moiety to the zirconium centre, we performed detailed Bader analysis^[26] of compounds **3a,b**. Scherer and McGrady recently reported a very detailed investigation into the agostic bonding criteria of titanium ethyl compounds and we are using their criteria here to assign the bonding mode of the phenyl group.^[27–29] They extended the original definition of agostic bond (“used to discuss the various manifestations of covalent interactions between carbon–hydrogen groups and transition-metal centres in organometallic compounds, in which a hydrogen atom is covalently bonded simultaneously to both a carbon and to a transition-metal atom”^[30,31]) to a broader context (“agostic interactions are characterized by the distortion of an organometallic moiety which brings an appended C–H bond into close proximity with the metal centre”^[29]), and included heteroatoms such as silicon. Their main criterion for the definition of an agostic bond was the relationship of the electron density distribution $\rho(r)$ and the Laplacian of the charge density $\nabla^2\rho(r)$ in connection with Bader AIM analysis.^[26] To support these so-obtained results, we undertook a detailed NBO analysis to investigate the relevant orbitals that were involved in the coordination of the phenyl moiety.^[32]

For **3a**, we found a bonding path and a bond critical point between the zirconium centre and the *ortho* carbon of the phenyl group (BCP1). We did not observe a bonding path or a bond critical point between the zirconium centre and the hydrogen atom bonded to the *ortho* carbon (Figure 2). The electron density at the bond critical point was determined to be $\rho(r) = 0.0171$ and the Laplacian of the charge density $\nabla^2\rho(r) = -0.0136$. For comparison, the bond critical point between the zirconium centre and the CH_2 group (BCP2) was $\rho(r) = 0.0812$ and a Laplacian of $\nabla^2\rho(r) = -0.0165$ found. Obviously, as the electron density of BCP1 is lower than the electron density of the BCP2 bond,

we concluded that rather than a typical Lewis-type bond between the zirconium centre and the *ortho* carbon of the phenyl moiety, a more polarised bonding mode as we have previously described existed.^[16]

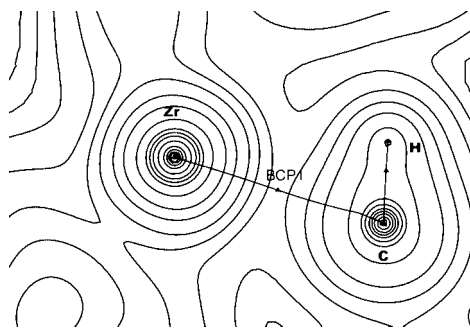


Figure 2. Contour plot of the electron density $\rho(r)$ of **3a**. Plane through zirconium, *ortho* phenyl carbon and hydrogen. Default contour lines used.

NBO analysis revealed electron donation between the CH bonding orbital [$\sigma_{CH} = 0.794(sp^{2.30})_C + 0.607(s)_H$] and the empty Zr orbital of mainly d-character ($LP^*_{Zr} = sd^{3.81}$) with a second-order perturbation energy of 5.12 kcal/mol. For comparison, for the CH bonding orbital in the *para* position of the coordinated carbon, similar values were obtained [$\sigma_{CH} = 0.794(sp^{2.34})_C + 0.608(s)_H$]. Thus, as the second-order perturbation energy for this carbon to zirconium is zero (i.e. no bond), we concluded that although there is a bonding path between the *ortho* carbon and the zirconium centre, the NHO of the two carbons are very similar, which indicates that an electrostatic rather than a covalent bond exists. Coloured plots of the orbitals are available in the Supporting Information (Figures S1–S3).

For **3b**, Bader analysis revealed a bonding path from the zirconium centre to the coordinated *ortho* carbon of the phenyl moiety; however, in this case, a straight line, as in **3a**, was not detected, but a more curved line was found (cf. Figure 3). It appears as if the bonding path first steers towards the bond critical point of the CH bond and just before it reaches this point it turns sharply towards the carbon atom. A similar kind of “conflict catastrophe structure” has been observed before, notably with alkyl titanium chloride cations^[33] and for unusual $H\cdots\pi$ interactions.^[34]

The relevant values of the bond critical point (BCP3) were calculated as $\rho(r) = 0.0114$ and $\nabla^2\rho(r) = -0.0086$. For comparison, the values of the bond critical point (BCP4) between the zirconium centre and the CH_2 group were calculated to be $\rho(r) = 0.0803$ and $\nabla^2\rho(r) = -0.0160$, which are similar to BCP2. The values for BCP1 are somewhat higher than the values of BCP3, which indicates a higher electron density between the zirconium centre and the *ortho* carbon of the phenyl moiety in the case of **3a**. NBO analysis of **3b** revealed the expected interaction between the CH bond [$\sigma_{CH} = 0.786(sp^{2.30})_C + 0.618(s)_H$] and the empty orbital ($LP^*_{Zr} = sd^{3.81}$) with a second-order perturbation energy of 3.09 kcal/mol, but furthermore, an interaction between the C–C bond [$\pi_{CC} = 0.675(p)_{C-ipso} + 0.738(p)_{C-ortho}$] with an energy of 5.88 kcal/mol (cf. Figures S4–S7). For

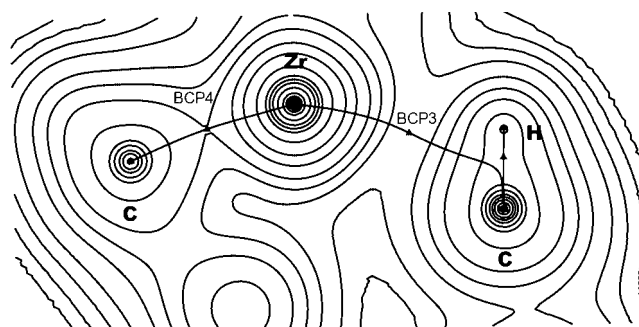


Figure 3. Contour plot of the electron density $\rho(r)$ of **3b**. Plane through zirconium, *ortho*-phenyl carbon and hydrogen. Benzyl CH_2 is on the left hand side. Default contour lines used.

comparison, the second C–C bond between the *ipso* and the *ortho* carbon bond [$\pi_{CC} = 0.716(p)_{C-ipso} + 0.699(p)_{C-ortho}$] only has an energy of 1.21 kcal/mol. It is tempting to assign this coordination to *agostic coordination*; however, unlike in the cases reported by Scherer and McGrady, we did not find a bonding path between the zirconium centre and the hydrogen atom. It is possible that by replacing the benzyl moiety with a stronger donor this could be shifted towards agostic bonding. Owing to the curvature of the bonding path in **3b**, we concluded that, in this case, a “transition state” somewhere in between a covalent bond and an agostic bond must be present.

Chemical Shift Computations

To verify our computed structures with experimental results, we calculated the chemical shifts of **3a** and **3b**. Because of the low activation barrier between **3a** and **3b** (5.28 kcal/mol), we can assume that both compounds are in equilibrium even at -60°C . Furthermore, we predict a chemical shift of $\delta_H = 2.64$ ppm for the *ortho* hydrogen of the phenyl moiety. This unusual highfield shift for an aromatic hydrogen can be explained very easily because of the magnetic anisotropy cone of the η^2 -bonded benzyl moiety. This cone points straight to the *ortho* hydrogen of the phenyl moiety, and thus explains the unusual shift for an aromatic hydrogen. Similar observations have been made before.^[18] The experimental and calculated shifts are summarised in Table 3.

Low-Temperature VT-NMR Studies

The reaction between **2** and $B(C_6F_5)_3$ in CD_2Cl_2 was monitored by NMR spectroscopy (Figure 4). The spectrum recorded at -60°C indicates the coordination of both the tolyl and benzyl moieties. The chemical shift of the benzylic CH_2 group at $\delta_H = 2.69$ ppm and $\delta_{C\{H\}} = 45.5$ ppm together with the coupling constant $J_{C,H} = 149.0$ Hz clearly indicate an η^2 -coordinated benzyl moiety.^[35,36] The chemical shift of the diastereotopic CMe_2 groups at 1.05 and 1.62 ppm are indicative of coordination of the tolyl moiety. Similar values, albeit with a smaller difference, have been reported before.^[18] As predicted, a peak at $\delta_H = 2.33$ ppm

Table 3. Chemical shifts for **2** (observed) and **3a,b** (calculated).

	2		3a ^[c]		3b ^[c]	
	¹ H (δ [ppm]) ^[a]	¹³ C (δ [ppm]) ^[b]	¹ H (δ [ppm])	¹² C (δ [ppm])	¹ H (δ [ppm])	¹³ C (δ [ppm])
Ph ¹		137.7		140.0		139.4
Ph ²	2.33	98.2	2.64	103.2	7.25	128.7
Ph ³	6.72	136.4	6.59	142.0	7.91	139.8
Ph ⁴	—	—	—	128.5	—	131.3
Ph ⁵	7.67	130.0	7.82	141.6	6.71	134.7
Ph ⁶	7.13	126.5	7.04	128.3	5.46	108.8
CH ₂	2.96	45.5	3.27	48.6	3.36	56.5
	3.04	—	3.39	—	2.98	—
Ph ⁸	—	123.2	—	124.6	—	134.7
Ph ⁹	6.71	128.1	7.25	140.5	5.38	104.8
Ph ¹⁰	6.91	127.9	7.65	131.4	6.02	132.7
Ph ¹¹	6.84	122.9	7.75	133.0	7.15	130.8
Ph ¹²	6.91	127.9	7.67	131.6	7.67	136.1
Ph ¹³	6.71	128.1	7.16	135.7	7.37	137.4
CCH ₃	1.05	27.5	—	—	—	—
	1.62	26.8	—	—	—	—
CCH ₃	—	37.3	—	—	—	—
PhCH ₃	2.39	20.7	—	—	—	—
Cp	5.39	109.8	5.34	111.8	5.77	112.5
Cp'	5.22	97.7	5.26	99.9	5.94	101.8
	6.18	103.6	6.26	108.6	6.10	114.5
	5.79	106.4	5.88	109.1	6.18	111.3
	6.66	115.8	6.58	117.9	6.71	117.6

[a] −60 °C, CD₂Cl₂, 500 MHz. [b] −60 °C, CD₂Cl₂, 125 MHz. [c] B3LYP/IGLOII.

can be assigned to the *ortho* hydrogen of the coordinated tolyl moiety. The predicted equilibrium between **3a** and **3b** could be confirmed by EXSY spectroscopy (Figure 5). The

cross peak between $\delta_{\text{H}} = 2.33$ ppm and $\delta_{\text{H}} \approx 7.2$ ppm can only be explained by the interconversion between **3a** and **3b**, and fits very well with the predicted values of 2.64 and

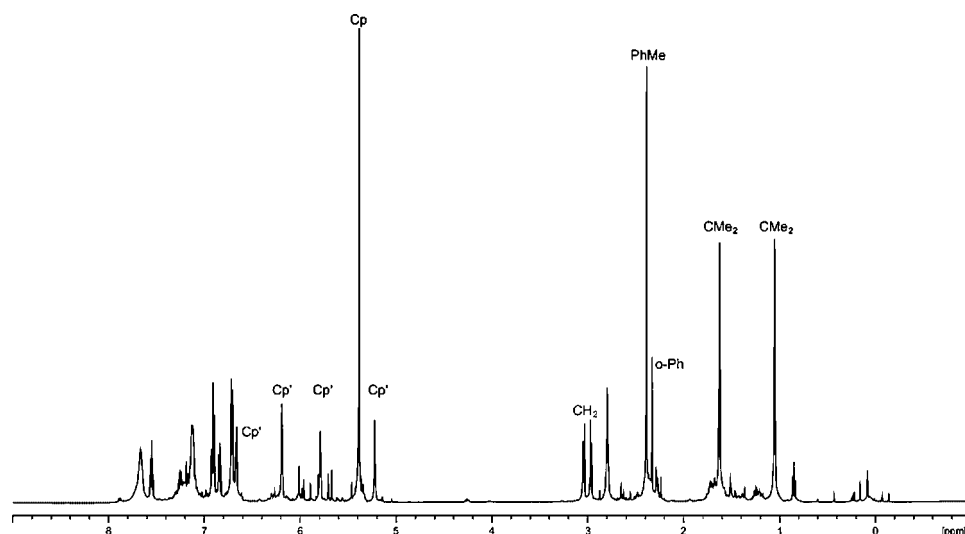


Figure 4. 500 MHz ¹H NMR spectrum of **2** at −60 °C. Significant peaks of the cation are labelled.

7.25 ppm.^[37] As expected, this exchange is rapid, even at -60°C , and thus some broad peaks in the aromatic region of the spectrum can be observed. Lowering the temperature to -90°C did not resolve the broad peaks, which hampered a detailed kinetic investigation. All calculated and observed chemical shifts are summarised in Table 3.

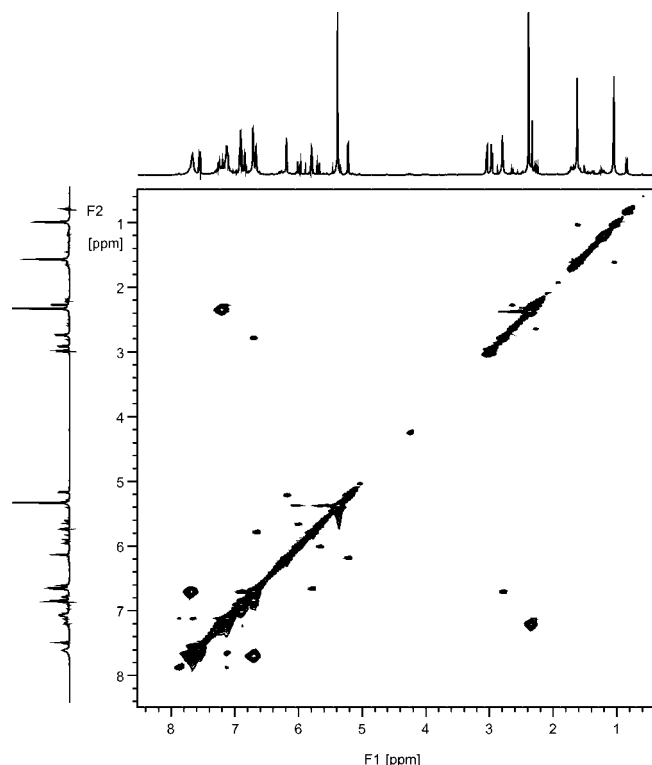


Figure 5. EXSY spectrum of **2** at -60°C in CD_2Cl_2 . Strong cross peaks are EXSY, medium ones are NOSY.

Conclusions

We prepared the benzyl congener $[\eta^5\text{-C}_5\text{H}_5\text{-(}\eta^5\text{-C}_5\text{H}_4\text{CMe}_2\text{C}_6\text{H}_4\text{Me)Zr(CH}_2\text{Ph)}_2]$ (**1**) of the previously reported zirconocene compound $[\eta^5\text{-C}_5\text{H}_5(\eta^5\text{-C}_5\text{H}_4\text{-CMe}_2\text{C}_6\text{H}_4\text{Me)ZrMe}_2]$. The reaction of **1** with $\text{B(C}_6\text{F}_5)_3$ in CD_2Cl_2 was monitored by low-temperature NMR spectroscopy, and we obtained evidence for the coordination of both the benzyl moiety in the expected and previously reported η^2 -bonding mode and the tolyl moiety. Our experimentally obtained data were predicted correctly from our computational studies. Furthermore, our model system predicted correctly the unusual chemical shift of $\delta_{\text{H}} = 2.33$ ppm (observed) and $\delta_{\text{H}} = 2.64$ ppm (calculated) for the *ortho* hydrogen of the coordinated tolyl (phenyl) moiety. Detailed AIM and NBO analysis revealed that although it is tempting to name this coordination “agostic”, strictly spoken it is not agostic but rather an electrostatic interaction for **3a**. For **3b**, this coordination mode can be best described as a “transition state” between a covalent bond an agostic bond. These results fit quite well with the reported bonding modes of Ti(Et)Cl_3 and dmpeTi(Et)Cl_3 : only in the case of the dmpe adduct could agostic bonding of the Et moiety be

observed. Our model clearly indicates that for styrene polymerisation with *ansa* group 4 metallocenes, the coordination of the phenyl ring from the growing chain does not hamper the coordination of the free monomer: it is possible for the monomer to get caught by the catalyst, rearrange and insert into the polymer chain.

Experimental Section

General: All experiments were carried out under a nitrogen atmosphere by using standard Schlenk techniques. Solvents were dried with sodium (toluene, low in sulfur), sodium/potassium alloy (diethyl ether, light petroleum, b.p. $40\text{--}60^{\circ}\text{C}$, pentane), potassium (thf) and calcium hydride (dichloromethane). All chemicals were purchased from Aldrich and used as received. NMR solvents were dried with activated molecular sieves, freeze thawed and stored in Young's Tap sealed ampoules. NMR spectra were recorded with a VARIAN Unity Plus 500 spectrometer and referenced to the residual proton solvent peak for ^1H . Chemical shifts are quoted in ppm relative to tetramethylsilane. ^{13}C NMR spectra were referenced with the solvent peak relative to tetramethylsilane and were proton decoupled by using a WALTZ sequence. CH coupling constants were measured with a coupled gHSQC pulse sequence. Low-temperature NMR studies were conducted as previously reported.^[19]

Computational Details: Density functional theory calculations were carried out by using the GAUSSIAN03^[38] program package, running on a Mandrake Linux Dual-Opteron or a Dual-Xeon system, respectively. Geometries were fully optimised without symmetry constraints, which involved the functional combinations according to Becke^[39] (hybrid) and Lee, Yang and Parr^[40] (denoted B3LYP), with the corresponding pseudopotential basis set for Zr (Stuttgart-Dresden, keyword SDD in Gaussian) and the standard 6-31G* basis set^[41] for C, H, Cl and F (denoted as ECP1). The stationary points and transition states were characterised as minima by analytical harmonic frequencies (zero or one imaginary frequency, respectively), which were used without scaling for zero-point and thermal corrections.

Magnetic shieldings σ were evaluated for the B3LYP/ECP1 geometries by using a recent implementation of the GIAO (gauge-including atomic orbitals)-DFT method,^[42] which involved the same B3LYP level of theory, together with the recommended IGLO II basis^[43] on C, H and F. The former approach with this particular combination of functionals and basis sets has proven to be quite effective for chemical shift computations for transition metal complexes.^[16] ^1H and ^{13}C NMR chemical shifts were calculated relative to benzene, with absolute shieldings for benzene $\sigma(^1\text{H})$ 24.54 and $\sigma(^{13}\text{C})$ 47.83 with the IGLO II basis set. The values for benzene were converted into the TMS scale by using the experimental δ values of benzene ($\delta = 7.26$ ppm and 128.5 ppm, respectively). Bader analysis was performed using the DZVP all-electron basis set,^[44] drawing of the electron charge density plots were performed with the use of an Aim2000 instrument.^[45] MOLDEN^[46] was used for the chemical representation of the calculated compounds and NBO-View for the representation of the orbitals.^[32]

$[\eta^5\text{-C}_5\text{H}_5\text{-(}\eta^5\text{-C}_5\text{H}_4\text{CMe}_2\text{C}_6\text{H}_4\text{Me)Zr(CH}_2\text{Ph)}_2]$ (1**):** Previously prepared $[\eta^5\text{-C}_5\text{H}_5\text{-(}\eta^5\text{-C}_5\text{H}_4\text{CMe}_2\text{C}_6\text{H}_4\text{Me)ZrCl}_2]$ ^[17] (2.4 g, 5.65 mmol) was added to a rapidly stirred solution of benzylmagnesium chloride in diethyl ether.^[20] The colour of the solution changed to orange. The reaction mixture was stirred overnight. The volatiles were removed under reduced pressure, and the orange residue was extracted into pentane. Fractionated crystallisation yielded

the desired compound in a moderate yield as orange microcrystals. Yield: 410 mg (13.5%). ^1H NMR (500 MHz, CDCl_3 , 20 °C): δ = 1.51 (s, 6 H, CCH_3), 1.82 (s, 4 H, $\text{CH}_2\text{-Ph}$), 2.24 (2, 3 H, PhCH_3), 5.71 (s, 5 H, Cp), 5.76 (apparent t, J = 5 Hz, 2 H, Cp'), 5.87 (apparent t, J = 5 Hz, 2 H, Cp'), 6.76 (t, J = 10 Hz, 2 H, $p\text{-H-Ph}$), 7.05 (d, J = 10 Hz, 4 H, $o\text{-H-Ph}$), 7.06 (d, J = 10 Hz, 4 H, $-C_4H_4\text{-Me}$), 7.09 (t, J = 10 Hz, 4 H, $m\text{-H-Ph}$) ppm. ^{13}C NMR (125 MHz, CDCl_3 , 20 °C): δ = 21.1 ($-C_4H_4\text{-CH}_3$), 30.9 (CCH_3), 39.7 (CCH_3), 61.4 ($\text{CH}_2\text{-}$), 111.8 (Cp'), 112.8 (Cp), 120.9 ($p\text{-C-Ph}$), 125.7 ($o\text{-C-Ph}$), 126.2 ($o\text{-C-tolyl}$), 128.2 ($m\text{-C-Ph}$), 129.1 ($m\text{-C-tolyl}$), 136.0 ($is\text{po-C}$), 138.3 ($is\text{po-C}$), 146.7 ($is\text{po-C}$), 152.5 ($is\text{po-C}$) ppm. $\text{C}_{34}\text{H}_{36}\text{Zr}$ (535.59): calcd. C 76.21, H 6.77; found C 76.10, H 6.65.

Supporting Information (see footnote on the first page of this article): Coloured plots of the NBO of **3a,b** and tables of the cartesian coordinates of all calculated structures in x, y, z format.

Acknowledgments

J. S. thanks J. C. Green, M. Bühl and M. Flock for helpful discussions and F. Stelzer for his support. A. T. thanks the Technical University of Graz for a research grant. We want to thank the IT department for computational resources.

- [1] M. S. W. Chan, K. Vanka, C. C. Pye, T. Ziegler, *Organometallics* **1999**, *18*, 4624–4636.
- [2] K. Vanka, M. S. W. Chan, C. C. Pye, T. Ziegler, *Organometallics* **2000**, *19*, 1841–1849.
- [3] K. Vanka, T. Ziegler, *Organometallics* **2001**, *20*, 905–913.
- [4] K. Vanka, Z. Xu, M. Seth, T. Ziegler, *Top. Catal.* **2005**, *34*, 143–164.
- [5] S.-Y. Yang, T. Ziegler, *Organometallics* **2006**, *25*, 887–900.
- [6] M. Bochmann, *J. Chem. Soc., Dalton Trans.* **1996**, 255–270.
- [7] M. Bochmann, *Top. Catal.* **1999**, *7*, 9–22.
- [8] M. Bochmann, *J. Organomet. Chem.* **2004**, *689*, 3982–3998.
- [9] M. Bochmann, G. J. Pindado, S. J. Lancaster, *J. Mol. Catal. A* **1999**, *146*, 179–190.
- [10] H.-H. Brintzinger, D. Fischer, R. Mühlhaupt, B. Rieger, R. Waymouth, *Angew. Chem.* **1995**, *107*, 1255–1383.
- [11] G. J. P. Britovsek, V. C. Gibson, D. F. Wass, *Angew. Chem. Int. Ed.* **1999**, *38*, 428–447.
- [12] E. Y.-X. Chen, T. J. Marks, *Chem. Rev.* **2000**, *100*, 1391–1434.
- [13] W. Kaminsky, *J. Polym. Sci., Part A: Polym. Chem.* **2004**, *16*, 3911–3921.
- [14] A. Maccioni, *Chem. Rev.* **2005**, *105*, 2039–2073.
- [15] G. L. Rempel, J. Huang, *Prog. Polym. Sci.* **1995**, *20*, 459–526.
- [16] M. Bühl, J. Saßmannshausen, *J. Chem. Soc., Dalton Trans.* **2001**, 79–84.
- [17] L. H. Doerrer, M. L. H. Green, D. Häußinger, J. Saßmannshausen, *J. Chem. Soc., Dalton Trans.* **1999**, 2111–2118.
- [18] M. L. H. Green, J. Saßmannshausen, *Chem. Commun.* **1999**, 115–116.
- [19] J. Saßmannshausen, J. C. Green, F. Stelzer, J. Baumgartner, *Organometallics* **2006**, *25*, 2796–2805.
- [20] J. Saßmannshausen, A. Track, F. Stelzer, *Organometallics* **2006**, *25*, 4427–4432.
- [21] N. Ishihara, T. Seimiya, M. Kuramono, M. Uoi, *Polym. Prepr. Jpn.* **1986**, *35*, 240.
- [22] C. Schwecke, W. Kaminsky, *J. Polym. Sci., Part A: Polym. Chem.* **2001**, *39*, 2805–2812.
- [23] Q. Wang, R. Quyoum, D. J. Gillis, M.-J. Tudoret, D. Jeremic, B. K. Hunter, M. C. Baird, *Organometallics* **1996**, *15*, 693–703.
- [24] J. H. Yang, J. Huh, W. H. Jo, *Organometallics* **2006**, *25*, 1144–1150.
- [25] M. Bochmann, M. L. H. Green, A. K. Powell, J. Saßmannshausen, M. U. Triller, S. Wocadlo, *J. Chem. Soc., Dalton Trans.* **1999**, 43–49.
- [26] R. F. W. Bader, *Atoms in Molecules: A Quantum Theory*, Clarendon Press, Oxford, UK, **1990**.
- [27] W. Scherer, W. Hieringer, M. Spiegler, P. Sirsch, G. S. McGrady, A. J. Downs, A. Haarland, B. Pedersen, *Chem. Commun.* **1998**, 2471–2472.
- [28] W. Scherer, P. Sirsch, D. Shorokhov, M. Tafipolsky, G. S. McGrady, E. Gullo, *Chem. Eur. J.* **2003**, *9*, 6057–6070.
- [29] W. Scherer, G. S. McGrady, *Angew. Chem. Int. Ed.* **2004**, *43*, 1782–1806.
- [30] M. Brookhard, M. L. H. Green, *J. Organomet. Chem.* **1983**, *250*, 395–408.
- [31] M. Brookhart, M. L. H. Green, L.-L. Wong, *Prog. Inorg. Chem.* **1988**, *36*, 1–124.
- [32] E. D. Glendening, J. K. Badenhoop, A. E. Reed, J. E. Carpenter, J. A. Bohmann, C. M. Morales, F. Weinhold in *NBO 5.0*, Theoretical Chemistry Institute, University of Wisconsin, Madison, WI, **2001**.
- [33] P. L. A. Popelier, G. Logothetis, *J. Organomet. Chem.* **1998**, *555*, 101–111.
- [34] I. Rozas, I. Alkorta, J. Elguero, *J. Phys. Chem. A* **1997**, *101*, 9457–9463.
- [35] R. F. Jordan, R. E. LaPointe, N. C. Baenzinger, G. D. Hinch, *Organometallics* **1990**, *9*, 1539–1545.
- [36] R. F. Jordan, R. E. LaPointe, C. S. Bajgur, S. F. Echols, R. Willet, *J. Am. Chem. Soc.* **1987**, *109*, 4111–4113.
- [37] A cross peak between the two methyl groups on the bridging carbon should also be observed. However, the chemical shift difference between the two isomers is probably too small to be observed. For our model compound, we computed a difference around 0.5 ppm.
- [38] M. J. Frisch, G. W. Trucks, H. B. Schlegel, G. E. Scuseria, M. A. Robb, J. R. Cheeseman, J. A. Montgomery Jr, T. Vreven, K. N. Kudin, J. C. Burant, J. M. Millam, S. S. Iyengar, J. Tomasi, V. Barone, B. Mennucci, M. Cossi, G. Scalmani, N. Rega, G. A. Petersson, H. Nakatsuji, M. Hada, M. Ehara, K. Toyota, R. Fukuda, J. Hasegawa, M. Ishida, T. Nakajima, Y. Honda, O. Kitao, H. Nakai, M. Klene, X. Li, J. E. Knox, H. P. Hratchian, J. B. Cross, C. Adamo, J. Jaramillo, R. Gomperts, R. E. Stratmann, O. Yazyev, A. J. Austin, R. Cammi, C. Pomelli, J. W. Ochterski, P. Y. Ayala, K. Morokuma, G. A. Voth, P. Salvador, J. J. Dannenberg, V. G. Zakrzewski, S. Dapprich, A. D. Daniels, M. C. Strain, O. Farkas, D. K. Malick, A. D. Rabuck, K. Raghavachari, J. B. Foresman, J. V. Ortiz, Q. Cui, A. G. Baboul, S. Clifford, J. Cioslowski, B. B. Stefanov, G. Liu, A. Liashenko, P. Piskorz, I. Komaromi, R. L. Martin, D. J. Fox, T. Keith, M. A. Al-Laham, C. Y. Peng, A. Nanayakkara, M. Challacombe, P. M. W. Gill, B. Johnson, W. Chen, M. W. Wong, C. Gonzalez, J. A. Pople, *Gaussian 03, Revision C.02*, Gaussian, Inc., Pittsburgh, PA, **2004**.
- [39] A. D. Becke, *J. Chem. Phys.* **1993**, *98*, 5648–5652.
- [40] C. Lee, W. Yang, R. G. Parr, *Phys. Rev. B* **1988**, *37*, 785–789.
- [41] W. J. Hehre, R. Ditchfield, J. A. Pople, *J. Chem. Phys.* **1972**, *56*, 2257–2261.
- [42] J. R. Cheeseman, G. W. Trucks, T. A. Keith, M. J. Frisch, *J. Chem. Phys.* **1996**, *104*, 5497–5509.
- [43] W. Kutzelnigg, U. Fleischer, M. Schindler in *NMR Basic Principles and Progress Vol. 23*, Springer, Berlin, **1990**, pp. 165–262.
- [44] N. Godbout, D. R. Salahub, J. Andzelm, *Can. J. Chem.* **1992**, *70*, 560.
- [45] F. Biegler-König, J. Schönbohm, D. Bayles, *J. Comput. Chem.* **2001**, *22*, 545–559.
- [46] G. Schaftenaar, J. H. Noordik, *J. Comput. Aided Mol. Des.* **2000**, *14*, 123–134.

Received: January 2, 2007

Published Online: April 18, 2007